ACS APPLIED OPTICAL MATERIALS

pubs.acs.org/acsaom Letter

Tunable Broadband Molecular Emission in Mixed-Organic-Cation Two-Dimensional Hybrid Perovskites

YunHui L. Lin and Justin C. Johnson*

Cite This: ACS Appl. Opt. Mater. 2023, 1, 3−9 Read Online

ACCESS | Metrics & More | Article Recommendations | Supporting Information

ABSTRACT: The ability to controllably enhance or suppress the luminescence contributions from different species in layered two-dimensional (2D) hybrid perovskites is beneficial for developing color-tunable broadband emitters. In particular, for 2D perovskites exhibiting interlayer sensitized triplet emission from their organic cations, the final molecular emission profiles are often influenced by intermolecular interactions between neighboring chromophores. Embedding these chromophores within an inert host cation is an emerging strategy for controlling the degree of intermolecular coupling and thereby influencing the formation of isolated monomer versus multimolecular states. In this work, we demonstrate tunable broadband emission from 2D perovskites containing varying amounts of a naphthalene chromophore mixed with hexylammonium cations. Across the series of perovskites, emission from free or self-trapped excitons and naphthalene triplet monomers or excimers contributes to wide color tunability from green to yellow to orange. These results suggest that organic-cation mixing may be a generalizable approach for modifying photophysical outcomes in 2D hybrid perovskites.

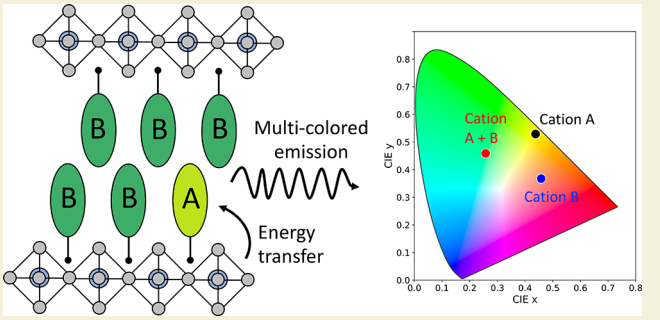

KEYWORDS: *excitons, perovskites, layered materials, energy transfer, phosphorescence, excimer, triplet sensitization, hybrid interfaces*

INTRODUCTION

The emission properties of layered two-dimensional (2D) metal halide perovskites can be widely tuned through compositional or structural control.[1] In particular, their luminescence profiles can vary from narrow to broadband due to a diversity of emission sources, including free or self-trapped excitons in the inorganic layer,[2−4] defect states,[5−7] and certain molecular species in the organic layer.[8−11] This remarkable spectral tunability has made 2D perovskites valuable as single-phase bulk emitters with applications in solid-state lighting or commercial displays.

One of the ways to achieve broadband luminescence in 2D perovskites is by inducing emission from the triplet states of optically active ammonium-linked organic cations that are embedded in the 2D perovskite structure. This organic phosphorescence is activated through an interlayer triplet sensitization process across the inorganic metal halide−organic cation interface.[12,13] Ruddlesden−Popper 2D hybrid perovskites with an A_2BX_4 chemical formula are self-assembled, natural quantum well structures comprised of anionic single layers of metal halide octahedra $[BX_6]^{4-}$ separated by cationic double layers of organic spacer molecules $[A]^+$. Stable excitons are formed within the inorganic framework at room temperature,[14] and the presence of heavy metal (e.g., Pb^{2+} or Sn^{2+}) and halide (e.g., Cl^-, Br^-, or I^-) atoms allows effective mixing of their spin states.[15] Under certain conditions, these inorganic excitons can act as photosensitizers for molecular triplets in the adjacent organic spacer layer.

Typically, to obtain the necessary energy level alignment to drive triplet energy transfer between the inorganic metal halide exciton and the organic-cation states, conjugated organic chromophores with low-lying triplet levels are needed.[16,17] However, a side effect of employing conjugated molecules in the 2D perovskite structure is that the final luminescence profiles of the perovskite are often dominated by multimolecular species such as excimers.[11,18,19] These multimolecular species can be difficult to avoid due to the extended π-networks that arise when conjugated molecules are packed closely in the solid state. While broadband emission from multimolecular or aggregation-induced states may be desirable in its own right,[10,20] in other situations, it is useful to gain control of the overall luminescence profile by tuning the relative emission contributions from isolated monomer states, multimolecular states, or other emissive species. Such control

Received: September 27, 2022
Accepted: October 28, 2022
Published: November 2, 2022

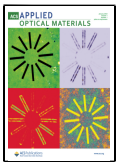

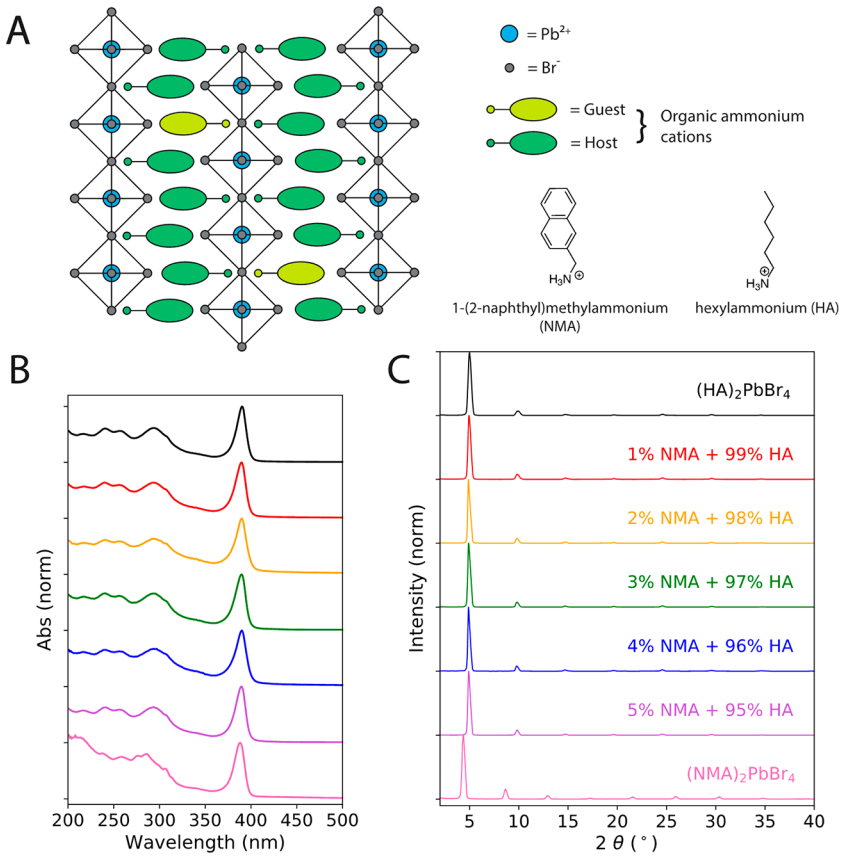

Figure 1. (A) Schematic of the single-layer 2D hybrid perovskite and molecular structure of the organic ammonium cations used in this study. (B) Absorption spectra of the 1-(2-naphthylmethyl) ammonium (NMA), hexylammonium (HA), and mixed HA/NMA lead bromide perovskite thin films. Spectra are normalized at the exciton transition near 390 nm and offset. (C) X-ray diffractograms of the perovskite thin films. Panels B and C share the same legend.

would enable systematic color tunability from the perovskite that is valuable for many light-emitting applications.

Organic guest/host mixing is a well-known strategy for suppressing chromophore/chromophore interactions. When the "guest" chromophore is embedded within a "host" matrix of inert wide-bandgap molecules, excited states of the guest are protected against quenching interactions with their environment.[21] In the 2D perovskite community, organic-cation mixing has been employed to extend the phosphorescence lifetime or to improve the room-temperature luminescence yield of the emissive chromophores.[22−24] Maintaining phase-pure and crystalline environments requires matching of the guest and host molecular geometric profiles (e.g., pentacene and *p*-terphenyl),[25] which adds constraints on the types of hosts that can be used.

We synthesized a series of Ruddlesden−Popper 2D hybrid perovskite thin films containing mixed aromatic and alkyl-ammonium cations and studied their photophysical properties. While the emission of the purely aromatic-containing perovskite is dominated by molecular triplet excimers and the emission of the purely alkyl-containing perovskite is dominated by inorganic free and self-trapped excitons, the mixed-cation systems exhibit unique luminescence behavior stemming from guest−host interactions between the aromatic and alkyl molecules. Consequently, multicolored emission is achieved across this series of films due to different relative contributions from inorganic free or self-trapped excitons and molecular triplet monomers or excimers. The assignment of the spectral features is corroborated by time-resolved photoluminescence measurements that, at early time scales, reveal a rapid decay of the inorganic exciton emission coupled with a rise time in the molecular emissions that is consistent with interlayer energy transfer. Subsequently, the molecular species exhibit long-lived decays that are typical of triplet-based emissions. Ultimately, these findings suggest that organic-cation mixing between conjugated guest chromophores within an alkyl-ammonium host may be a generalized approach for controlling intermolecular interactions and thereby tuning the spectral properties of 2D hybrid metal halide perovskites.

RESULTS AND DISCUSSION

Using conventional solution processing techniques, we prepared a series of 2D hybrid perovskite thin films containing systematically mixed aromatic and alkyl-ammonium cations with a $(HA)_{2-x}(NMA)_xPbBr_4$ chemical formula. Within the organic layers, the alkyl-ammonium cation, hexylammonium (HA), serves as the insulating "host" while the aromatic cation, 1-(2-naphthylmethyl) ammonium (NMA), serves as the triplet acceptor "guest" and phosphorescent emitter (Figure 1A). HA, a linear alkyl-ammonium cation with a length comparable to that of NMA, was selected as the host molecule because combining two organic cations of similar length and cross-sectional shape promotes formation of a single mixed-cation phase and reduces the chance of perovskite segregation into pure-cation phases. Absorption and X-ray diffraction (XRD) measurements on the mixed films suggest that at low

https://doi.org/10.1021/acsaom.2c00106
ACS Appl. Opt. Mater. 2023, 1, 3−9

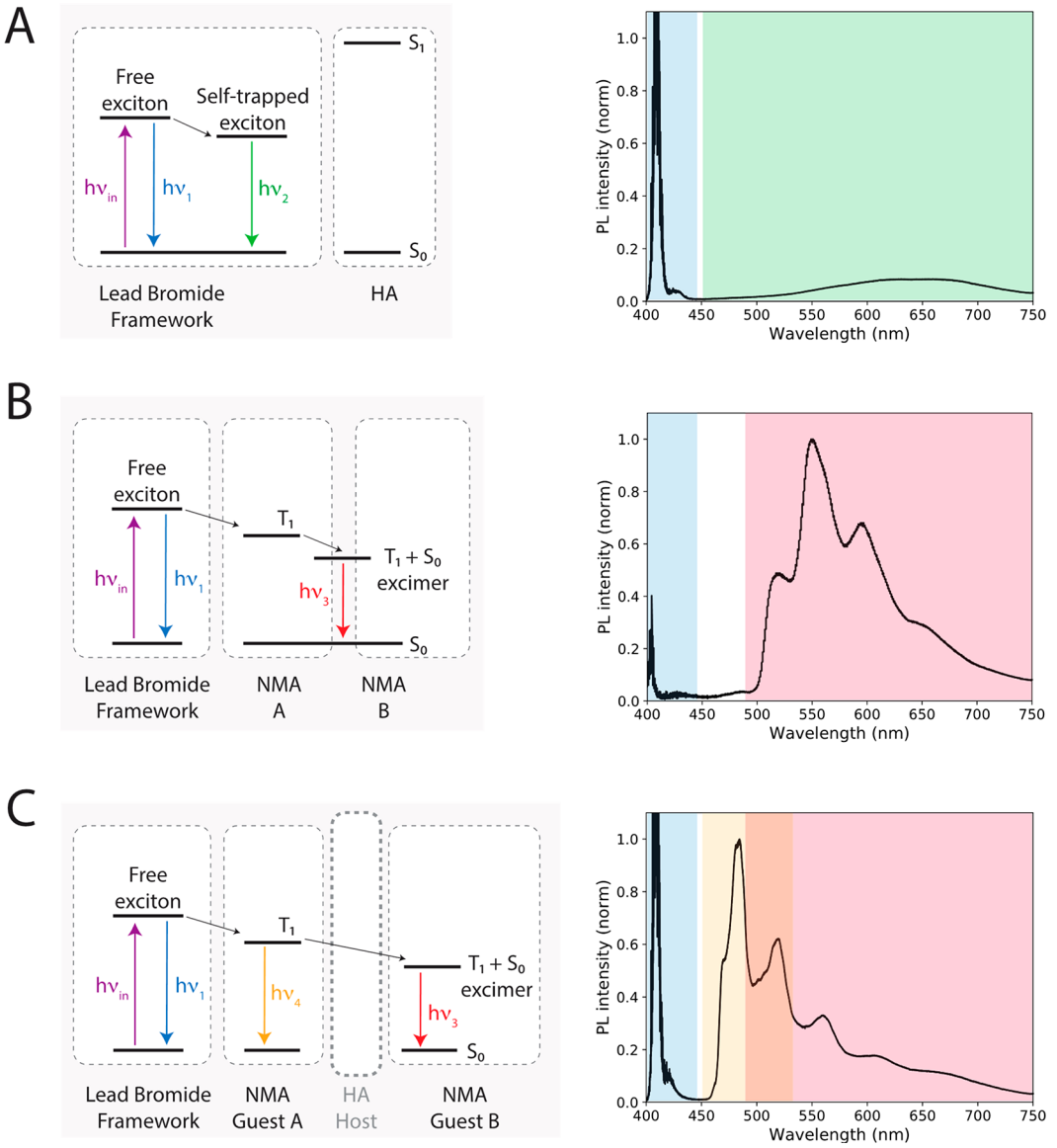

Figure 2. Key exciton transitions present in the (A) hexylammonium (HA), (B) 1-(2-naphthylmethyl) ammonium (NMA), and (C) mixed HA/NMA lead bromide perovskite thin films following photoexcitation of the lead bromide exciton band. Right panels show photoluminescence spectra of the samples measured at 77 K with different regions of the spectra shaded in the same color as the corresponding emissive species in the left Jablonski diagrams.

concentrations of NMA of <5 mol %, the organic layers are homogeneously mixed without obvious phase segregation of HA- and NMA-only perovskites. At higher molar concentrations of NMA, we observe two distinct reflections in the XRD data corresponding to pure HA and NMA perovskite phases, a clear indication of phase segregation (Figure S1).

The absorption spectra of the films are shown in Figure 1B, with both $(NMA)_2PbBr_4$ and $(HA)_2PbBr_4$ possessing similar exciton transitions that peak at 388 and 390 nm, respectively. Thin-film x-ray diffractograms of the compounds are shown in Figure 1C and exhibit equally spaced reflections typical of ⟨100⟩-oriented 2D perovskites.[26] The interlayer separation, evaluated from the diffraction peak positions, is 20.2 Å for the $(NMA)_2PbBr_4$ perovskite and 17.8 Å for the $(HA)_2PbBr_4$ perovskite (Table S1). Moreover, the diffraction peaks of the mixed HA/NMA compounds are systematically shifted between the lattice spacings of pure NMA and pure HA perovskite with no detectable peak separation, suggesting that the $(HA)_2PbBr_4$ perovskite lattice spacing is expanded slightly by the small quantities of NMA without disrupting the underlying layered structure.

The photoluminescence (PL) spectra of this series of perovskite compounds were measured at 77 K under 365 nm continuous-wave excitation, with results shown in Figure 2. The 365 nm excitation falls beyond the absorbance of both naphthalene and hexane molecules, ensuring that photoexcitations are initially localized within the lead bromide framework. In the $(HA)_2PbBr_4$ perovskite (Figure 2A), the PL spectrum is comprised of two emissive species, both originating from the inorganic lattice. First, direct recombination of the inorganic lead bromide excitons produces a sharp free exciton emission peak centered at 409 nm ($h\nu_1$, shaded blue region), representing a 148 meV Stokes shift relative to the exciton absorption peak centered at 390 nm. We note that while this Stokes shift is somewhat large in the context of inorganic semiconductors, shifts on the order of 100 meV are

https://doi.org/10.1021/acsaom.2c00106
ACS Appl. Opt. Mater. 2023, 1, 3−9

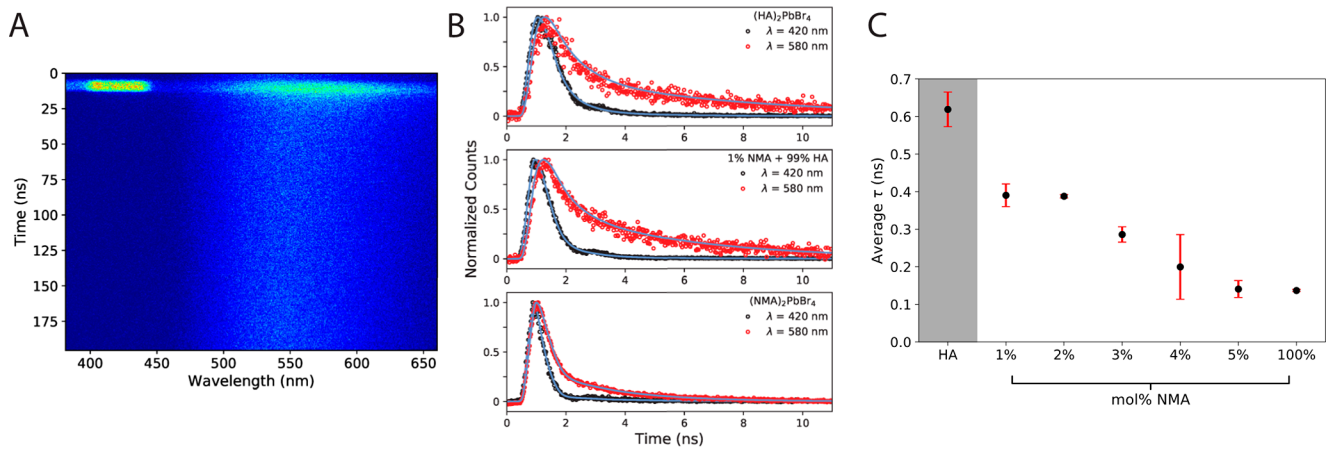

Figure 3. (A) Representative time-resolved PL streak camera image over a 200 ns time window, shown for the $(HA)_{1.9}(NMA)_{0.1}PbBr_4$ sample. (B) Early PL kinetics of the HA, 1% NMA/99% HA, and NMA perovskite thin films. The long-lived components have been subtracted from the 580 nm traces. The data were fitted using iterative reconvolution to the instrument response, with the fits colored blue. (C) Average time constant of the inorganic free exciton PL decays (center wavelength of 420 nm) as a function of the organic-cation composition.

not unusual for low-dimensional hybrid perovskites.[27] In addition to this free exciton emission, there is a less intense, broad, featureless, and highly red-shifted emission band between 500 and 750 nm ($h\nu_2$, shaded green region) due to recombination of self-trapped excitons. Self-trapped excitons are widely observed in hybrid metal halide perovskites due to their soft, deformable crystal lattices and strong electron−phonon coupling.[28]

In contrast to the $(HA)_2PbBr_4$ perovskite, the NMA-containing perovskites exhibit markedly different PL characteristics due to energy transfer between the inorganic and organic components. This interlayer energy transfer is made possible by a roughly 400 meV energetic driving force between the inorganic exciton and naphthalene triplet states,[19] and the mechanism for this interlayer triplet energy transfer has been described as either a Dexter-like process[29] or a sequential charge transfer process[11] in previous studies on naphthalene-containing lead bromide 2D perovskites. Like that of $(HA)_2PbBr_4$, the PL spectrum of $(NMA)_2PbBr_4$ (Figure 2B) contains a free exciton band centered at 405 nm. However, the intensity of this free exciton emission is strongly quenched compared to that of $(HA)_2PbBr_4$. The relatively weak free exciton emission is consistent with efficient energy transfer between the inorganic lead bromide exciton and naphthalene triplets. In addition to the weak free exciton emission, a more intense molecular emission is observed between 500 and 750 nm ($h\nu_3$, shaded red region) that is associated with naphthalene triplet excimers (i.e., a naphthalene triplet excited state coupled with a naphthalene ground-state molecule).[30] Due to the strong π-orbital interaction between naphthalene chromophores in $(NMA)_2PbBr_4$, triplet excimers are formed readily and represent the primary emissive species.

Finally, for the compounds containing both NMA and HA (Figure 2C), we observe relatively stronger inorganic free exciton emission centered at 410 nm that is consistent with less efficient interlayer energy transfer due to the reduced interfacial area between the lead bromide layers and naphthalene molecules. In addition to the free exciton emission, we observe intense naphthalene triplet monomer phosphorescence peaks around 470 nm ($h\nu_4$, shaded yellow region).[30] These naphthalene monomer emissions are absent in the $(NMA)_2PbBr_4$ compound and arise only as a consequence of the guest/host configuration in the mixed-cation systems. Because on average, in the mixed-cation compositions, a majority of naphthalene molecules are surrounded by insulating hexane species, the likelihood of triplet excimer formation is reduced. However, as shown in Figure 2C, triplet excimer emission is still present in the PL spectra of the mixed-cation compounds, albeit with lower intensity. It is likely that although guest/host mixing has significantly reduced the degree of naphthalene-to-naphthalene electronic coupling, there may still be small aggregates of naphthalene present in the perovskite structure (undetectable through absorption spectroscopy or XRD) that contribute to these excimeric emissions. Finally, given that interlayer energy transfer in the mixed-cation compounds is nonquantitative, it is possible that self-trapped excitons contribute to the broad emissions, as well. However, the strong luminescence signals from the naphthalene triplet species make this difficult to ascertain.

To understand the dynamics of interlayer energy transfer across the series, we captured the time-dependent luminescence of each sample at 77 K using a streak camera. A typical streak camera image over a 200 ns window is shown for a mixed-cation compound in Figure 3A. The free exciton emission centered around 410 nm exhibits a rapid, subnanosecond decay. On the contrary, the red-shifted emissions (ascribed to naphthalene triplet species and/or lead bromide self-trapped excitons, depending on the sample) exhibit multicomponent decays with fast and slow time constants. The long-lived components do not decay substantially within the largest time window (200 μs) available on our streak camera setup, so to visualize the fast decay processes, the long-lived components were subtracted as constant baselines fitted to the data at pre-excitation time points. Even though the inverse of the repetition rate of the laser was faster than these slow decays, such that some re-excitation may occur, because of the extreme differences in the time scales under investigation (<10 ns vs hundreds of microseconds), we do not expect these events to impact the interpretation of decays at short time scales.

When the free exciton PL decays were fitted to a biexponential model, each decay contained a major component with a time constant of several hundreds of picoseconds and a

https://doi.org/10.1021/acsaom.2c00106
ACS Appl. Opt. Mater. 2023, 1, 3−9

minor component with a time constant of several nanoseconds (Table S2). The average time constant for the series of perovskites is plotted in Figure 3C as a function of the organic-cation composition. Within the series, the inorganic free exciton in $(HA)_2PbBr_4$ decays the slowest, with an average time constant of 0.62 ns, and in $(NMA)_2PbBr_4$ decays the fastest, with an average time constant of 0.14 ns. For the mixed HA/NMA perovskites, the average rate of the decay trends with NMA content; the higher the percentage of NMA, the faster the inorganic exciton decay. Assuming similar radiative and nonradiative relaxation rates across the series of NMA-containing perovskites, the inorganic free exciton decay constant can be taken as a proxy for the rate of transfer of energy to naphthalene, making these trends consistent with the amount of lead bromide-to-naphthalene interfacial area that is available for the energy transfer process. Based on a kinetic analysis in which the radiative, nonradiative, and self-trapping rate constants are assumed to be equal for the $(HA)_2PbBr_4$ and NMA-containing samples, we estimate that the interlayer energy transfer efficiency ranges from 37% for $(HA)_{1.98}(NMA)_{0.02}PbBr_4$ to 78% for $(NMA)_2PbBr_4$ (section 4 of the Supporting Information).

Turning to the early dynamics of the red-shifted emissions in the range of 500−650 nm (red curves in Figure 3B), all decays exhibit a subtle rise time when compared to the instrument response and inorganic free exciton decays. For $(HA)_2PbBr_4$, this rise time reflects the exciton self-trapping process, whereas for NMA-containing samples, this rise time reflects energy transfer between the inorganic and organic components. While we were unable to capture accurate rise time constants for this component using a multiexponential reconvolution fit, their presence and trend with composition are evident from visual inspection of the decay traces. In particular, this rise time is most subtle for the $(NMA)_2PbBr_4$ perovskite, in which interlayer energy transfer is fastest. Finally, as shown in the full streak image in Figure 3A, the red-shifted molecular emissions in the NMA-containing compounds all possess a long-lived decay of >0.1 ms. These observations are corroborated by literature reports on related naphthalene lead bromide perovskites, in which triplet-based lifetimes on the order of several milliseconds have been measured.[11,29]

Having examined the photophysical properties of this series of 2D hybrid perovskites with mixed alkyl and aromatic organic cations, we now consider some practical applications of these materials and discuss opportunities for future study. By enabling control over emission contributions from different excited-state species, mixed-organic-cation 2D perovskites can function as color-tunable emitters. The wide color tunability of this particular series of HA- and NMA-containing 2D perovskites is exemplified by their CIE 1931 color coordinates, plotted in Figure 4. Within the series, broadband, multicolored emission from green to yellow to orange was achieved. The yellow emission of $(NMA)_2PbBr_4$ was easily visualized at room temperature, while the emissions of the other compounds were weakly visible at room temperature but became significantly brighter upon cooling to 77 K (Figure S4). The relative magnitudes of the inorganic free exciton PL versus molecular PL vary across the series of mixed HA/NMA perovskites (Figure S3), but as shown in Figure 4, the perceived color coordinates do not shift significantly within the green family. In future work, it may be possible to increase the spectral separation of the inorganic free exciton and molecular emission bands (for example, through a different choice of halides or molecular chromophores) to achieve greater color tunability, to target specific perceived colors, or to generate broadband white light emission. In this respect, the vast compositional space that is available to 2D hybrid perovskites offers a near continuum of potential targets for additional investigation.

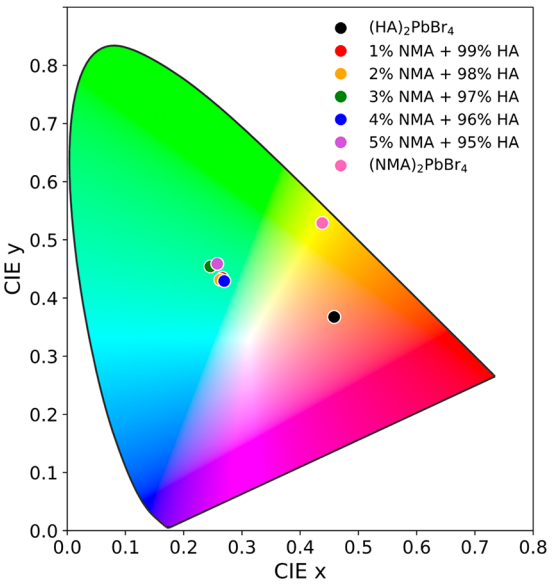

Figure 4. Chromaticity coordinates (CIE 1931) of the hexylammonium (HA), 1-(2-naphthylmethyl) ammonium (NMA), and mixed HA/NMA lead bromide perovskite emitters in this study.

Other useful applications of mixed-cation 2D hybrid perovskites stem from the ability to isolate the properties of individual phosphorescent chromophores from intermolecular effects. For example, several computational works have identified pairings of a metal halide with organic chromophores that are conducive to interlayer triplet energy flow,[16,17] but while such studies are valuable for the rapid screening of phosphorescent chromophores, they typically consider only the properties of the individual molecules. However, as this work and other experimental studies have shown, the excited-state behavior of 2D hybrid perovskites is highly susceptible to intermolecular interactions and depends sensitively on the organic layer morphology, which is not often considered computationally and may cause deviations from predictions based on isolated chromophore properties. Therefore, for a full understanding of photophysical outcomes in these materials, such computational studies must be coupled with perovskite crystal structure prediction and experimental verification. Whereas predicting and leveraging intermolecular interactions can provide a powerful set of tools for the design of emitters with targeted luminescence profiles, some of the complexities inherent to single-organic-cation systems can be simplified in mixed-organic-cation systems, where individual chromophores are insulated from intermolecular effects. In this way, the mixed-organic-cation architecture can serve as a valuable platform for fundamental studies of energy transfer at hybrid inorganic−organic interfaces.

CONCLUSION

In summary, we have demonstrated tunable broadband emission in a 2D hybrid perovskite by invoking a guest/host concept involving a phosphorescent conjugated organic chromophore embedded in a wide-bandgap alkylammonium

https://doi.org/10.1021/acsaom.2c00106
ACS Appl. Opt. Mater. 2023, 1, 3−9

host. Introducing <5 mol % phosphor within the alkyl host induces dramatic changes in the emission spectrum of the perovskite while maintaining a homogeneous mixed-cation phase. The dynamics of energy transfer among various species leads to an interesting interplay of excited-state behavior that we intend to characterize more incisively in future work involving pump−probe experiments. If well-understood, these principles can be extended to multiple phosphors to facilitate predictable energy flow and achieve even broader emission across the visible spectrum.

EXPERIMENTAL METHODS

Materials

To synthesize 1-(2-naphthylmethyl) ammonium bromide, 3 mmol (472 mg) of 1-(2-naphthyl) methylamine (Ark Pharm) was dissolved in 50 mL of ethanol and reacted with 3.6 mmol of HBr (48 wt % in water) by stirring for 1 h. The solvent was removed by evaporation, and the resulting white precipitate was rinsed several times in diethyl ether before drying overnight in a vacuum oven at 60 °C. Hexylammonium bromide was purchased from Great Cell Solar and used as is.

Film Preparation

Stock precursor solutions of $(NMA)_2PbBr_4$ and $(HA)_2PbBr_4$ were prepared by dissolving the organic ammonium bromide salts and $PbBr_2$ (Alfa Aesar) at a 2:1 molar ratio in dimethylformamide at 0.25 M with respect to lead. The mixed-organic-cation perovskite solutions were prepared by combining the $(NMA)_2PbBr_4$ and $(HA)_2PbBr_4$ stock solutions together in their nominal ratios. Thin films of the perovskites were spin coated at 4000 rpm for 40 s on precleaned glass or quartz substrates (for X-ray diffraction or optical measurements, respectively) and annealed at 100 °C for 10 min. All sample preparation was completed in a N_2 glovebox.

Characterization and Spectroscopy

Thin-film X-ray diffraction was performed using a Rigaku Ultima IV diffractometer using Cu Kα radiation. Absorption spectra were recorded using an Agilent Cary 6000i ultraviolet−visible−near infrared spectrophotometer with a diffuse reflectance attachment. Photoluminescence measurements were conducted on a Princeton Instruments spectrometer with PyLON CCD detectors. Samples were mounted in an Oxford Instruments sample-in-vapor liquid N_2 cryostat and excited with a 365 nm light-emitting diode filtered with a 10 nm bandpass filter. The detection arm was filtered with a 400 nm long pass filter. For accurate comparison of luminescence intensities across the broad detection range, intensity calibration was performed between 400 and 750 nm using a Princeton Instruments IntelliCal reference lamp. Time-resolved photoluminescence was measured using a Hamamatsu streak camera setup (model C10910-04). Samples were mounted in a Janis sample-in-vacuum liquid N_2 cryostat and excited with a PicoQuant 375 nm pulsed laser diode source. The full width at half-maximum of the instrument response was approximately 450 ps. Early dynamics (<10 ns) were measured with a repetition rate of 6.72 MHz, while late dynamics (<200 ns) were measured with a repetition rate of 1.9 MHz. The decay curves were fitted to the biexponential model $I(t) = A_1e^{-t/\tau_1} + A_2e^{-t/\tau_2} + y_0$ using an iterative reconvolution procedure with the instrument response. The amplitude average lifetimes were calculated with the equation $\tau_{avg} = (A_1\tau_1 + A_2\tau_2)/(A_1 + A_2)$.

ASSOCIATED CONTENT

Supporting Information

The Supporting Information is available free of charge at https://pubs.acs.org/doi/10.1021/acsaom.2c00106.

Additional X-ray diffraction data, PL spectra of the $(HA)_x(NMA)_{2-x}PbBr_4$ compounds, streak camera images, time-resolved PL decay curves, fitting parameters, and kinetic analysis (PDF)

AUTHOR INFORMATION

Corresponding Author

Justin C. Johnson − *National Renewable Energy Laboratory, Golden, Colorado 80401, United States;* orcid.org/0000-0002-8874-6637; Email: justin.johnson@nrel.gov

Author

YunHui L. Lin − *National Renewable Energy Laboratory, Golden, Colorado 80401, United States*

Complete contact information is available at: https://pubs.acs.org/10.1021/acsaom.2c00106

Notes

The authors declare no competing financial interest.

ACKNOWLEDGMENTS

Y.L.L. acknowledges support from the Director's Fellowship within NREL's Laboratory Directed Research and Development (LDRD) program. J.C.J. acknowledges support from the Solar Photochemistry Program of the U.S. Department of Energy, Office of Basic Energy Sciences, Division of Chemical Sciences, Biosciences, and Geosciences. This work was authored by Alliance for Sustainable Energy, LLC, the manager and operator of the National Renewable Energy Laboratory under Contract DE-AC36-08GO28308. The views expressed in the article do not necessarily represent the views of the Department of Energy or the U.S. Government. The U.S. Government retains and the publisher, by accepting the article for publication, acknowledges that the U.S. Government retains a nonexclusive, paid-up, irrevocable, worldwide license to publish or reproduce the published form of this work, or allow others to do so, for U.S. Government purposes.

REFERENCES

(1) Smith, M. D.; Connor, B. A.; Karunadasa, H. I. Tuning the Luminescence of Layered Halide Perovskites. *Chem. Rev.* **2019**, *119* (5), 3104−3139.

(2) Dohner, E. R.; Hoke, E. T.; Karunadasa, H. I. Self-Assembly of Broadband White-Light Emitters. *J. Am. Chem. Soc.* **2014**, *136* (5), 1718−1721.

(3) Stoumpos, C. C.; Cao, D. H.; Clark, D. J.; Young, J.; Rondinelli, J. M.; Jang, J. I.; Hupp, J. T.; Kanatzidis, M. G. Ruddlesden-Popper Hybrid Lead Iodide Perovskite 2D Homologous Semiconductors. *Chem. Mater.* **2016**, *28* (8), 2852−2867.

(4) Smith, M. D.; Karunadasa, H. I. White-Light Emission from Layered Halide Perovskites. *Acc. Chem. Res.* **2018**, *51* (3), 619−627.

(5) Wu, X.; Trinh, M. T.; Niesner, D.; Zhu, H.; Norman, Z.; Owen, J. S.; Yaffe, O.; Kudisch, B. J.; Zhu, X. Y. Trap States in Lead Iodide Perovskites. *J. Am. Chem. Soc.* **2015**, *137* (5), 2089−2096.

(6) Li, X.; Lian, X.; Pang, J.; Luo, B.; Xiao, Y.; Li, M. D.; Huang, X. C.; Zhang, J. Z. Defect-Related Broadband Emission in Two-Dimensional Lead Bromide Perovskite Microsheets. *J. Phys. Chem. Lett.* **2020**, *11* (19), 8157−8163.

(7) Yin, J.; Naphade, R.; Gutiérrez Arzaluz, L.; Brédas, J. L.; Bakr, O. M.; Mohammed, O. F. Modulation of Broadband Emissions in Two-Dimensional < 100>-Oriented Ruddlesden-Popper Hybrid Perovskites. *ACS Energy Lett.* **2020**, *5* (7), 2149−2155.

(8) Era, M.; Maeda, K.; Tsutsui, T. Enhanced Phosphorescence from Naphthalene-Chromophore Incorporated into Lead Bromide-Based Layered Perovskite Having Organic-Inorganic Superlattice Structure. *Chem. Phys. Lett.* **1998**, *296* (3−4), 417−420.

(9) Braun, M.; Tuffentsammer, W.; Wachtel, H.; Wolf, H. C. Pyrene as Emitting Chromophore in Organic-Inorganic Lead Halide-Based Layered Perovskites with Different Halides. *Chem. Phys. Lett.* **1999**, *307*, 373−378.
(10) Lim, C. K.; Maldonado, M.; Zalesny, R.; Valiev, R.; Ågren, H.; Gomes, A. S. L.; Jiang, J.; Pachter, R.; Prasad, P. N. Interlayer-Sensitized Linear and Nonlinear Photoluminescence of Quasi-2D Hybrid Perovskites Using Aggregation-Induced Enhanced Emission Active Organic Cation Layers. *Adv. Funct. Mater.* **2020**, *30* (16), 1909375.
(11) Tian, Y.; Li, Y.; Chen, B.; Lai, R.; He, S.; Luo, X.; Han, Y.; Wei, Y.; Wu, K. Sensitized Molecular Triplet and Triplet Excimer Emission in Two- Dimensional Hybrid Perovskites. *J. Phys. Chem. Lett.* **2020**, *11*, 2247.
(12) Lin, Y. L.; Blackburn, J. L.; Beard, M. C.; Johnson, J. C. Interlayer Triplet-Sensitized Luminescence in Layered Two-Dimensional Hybrid Metal-Halide Perovskites. *ACS Energy Lett.* **2021**, *6* (11), 4079−4096.
(13) Dong, Y.; Han, Y.; Chen, R.; Lin, Y.; Cui, B.-B. Recent Progress of Triplet State Emission in Organic-Inorganic Hybrid Metal Halides. *J. Lumin.* **2022**, *249*, 119013.
(14) Straus, D. B.; Kagan, C. R. Electrons, Excitons, and Phonons in Two-Dimensional Hybrid Perovskites: Connecting Structural, Optical, and Electronic Properties. *J. Phys. Chem. Lett.* **2018**, *9* (6), 1434−1447.
(15) Mondal, N.; De, A.; Seth, S.; Ahmed, T.; Das, S.; Paul, S.; Gautam, R. K.; Samanta, A. Dark Excitons of the Perovskites and Sensitization of Molecular Triplets. *ACS Energy Lett.* **2021**, *6* (2), 588−597.
(16) Leveillee, J.; Katan, C.; Even, J.; Ghosh, D.; Nie, W.; Mohite, A. D.; Tretiak, S.; Schleife, A.; Neukirch, A. J. Tuning Electronic Structure in Layered Hybrid Perovskites with Organic Spacer Substitution. *Nano Lett.* **2019**, *19* (12), 8732−8740.
(17) Wu, Y.; Lu, S.; Zhou, Q.; Ju, M.; Zeng, X. C.; Wang, J. Two-Dimensional Perovskites with Tunable Room- Temperature Phosphorescence. *Adv. Funct. Mater.* **2022**, *32*, 2204579.
(18) Papavassiliou, G. C.; Vidali, M. S.; Pagona, G.; Mousdis, G. A.; Karousis, N.; Koutselas, I. Effects of Organic Moieties on the Photoluminescence Spectra of Perovskite-Type Tin Bromide Based Compounds. *J. Phys. Chem. Solids* **2015**, *79*, 1−6.
(19) Lin, Y. L.; Johnson, J. C. Interlayer Triplet Energy Transfer in Dion - Jacobson Two- Dimensional Lead Halide Perovskites Containing Naphthalene Diammonium Cations. *J. Phys. Chem. Lett.* **2021**, *12*, 4793−4798.
(20) Wang, Y.; Yan, D.; Wang, L.; Wang, D.; Tang, B. Z. Aggregation-Induced Emission Luminogens Sensitized Quasi-2D Hybrid Perovskites with Unique Photoluminescence and High Stability for Fabricating White Light-Emitting Diodes. *Adv. Sci.* **2021**, *8*, 2100811.
(21) Guo, S.; Dai, W.; Chen, X.; Lei, Y.; Shi, J.; Tong, B.; Cai, Z.; Dong, Y. Recent Progress in Pure Organic Room Temperature Phosphorescence of Small Molecular Host-Guest Systems. *ACS Mater. Lett.* **2021**, *3* (4), 379−397.
(22) Hu, H.; Meier, F.; Zhao, D.; Abe, Y.; Gao, Y.; Chen, B.; Salim, T.; Chia, E. E. M.; Qiao, X.; Deibel, C.; Lam, Y. M. Efficient Room-Temperature Phosphorescence from Organic-Inorganic Hybrid Perovskites by Molecular Engineering. *Adv. Mater.* **2018**, *30* (36), 1707621.
(23) Hu, H.; Zhao, D.; Gao, Y.; Qiao, X.; Salim, T.; Chen, B.; Chia, E. E. M.; Grimsdale, A. C.; Lam, Y. M. Harvesting Triplet Excitons in Lead-Halide Perovskites for Room-Temperature Phosphorescence. *Chem. Mater.* **2019**, *31* (7), 2597−2602.
(24) Yang, S.; Wu, D.; Gong, W.; Huang, Q.; Zhen, H.; Ling, Q.; Lin, Z. Highly Efficient Room-Temperature Phosphorescence and Afterglow Luminescence from Common Organic Fluorophores in 2D Hybrid Perovskites. *Chem. Sci.* **2018**, *9* (48), 8975−8981.
(25) Lubert-Perquel, D.; Salvadori, E.; Dyson, M.; Stavrinou, P. N.; Montis, R.; Nagashima, H.; Kobori, Y.; Heutz, S.; Kay, C. W. M. Identifying Triplet Pathways in Dilute Pentacene Films. *Nat. Commun.* **2018**, *9*, 4222.
(26) Li, X.; Hoffman, J. M.; Kanatzidis, M. G. The 2D Halide Perovskite Rulebook: How the Spacer Influences Everything from the Structure to Optoelectronic Device Efficiency. *Chem. Rev.* **2021**, *121* (4), 2230−2291.
(27) Papavassiliou, G. C.; Mousdis, G. A.; Koutselas, I. B. Some New Organic-Inorganic Hybrid Semiconductors Based on Metal Halide Units: Structural, Optical and Related Properties. *Adv. Mater. Opt. Electron.* **1999**, *9*, 265−271.
(28) Li, S.; Luo, J.; Liu, J.; Tang, J. Self-Trapped Excitons in All-Inorganic Halide Perovskites: Fundamentals, Status, and Potential Applications. *J. Phys. Chem. Lett.* **2019**, *10* (8), 1999−2007.
(29) Ema, K.; Inomata, M.; Kato, Y.; Kunugita, H.; Era, M. Nearly Perfect Triplet-Triplet Energy Transfer from Wannier Excitons to Naphthalene in Organic-Inorganic Hybrid Quantum-Well Materials. *Phys. Rev. Lett.* **2008**, *100* (25), 1−4.
(30) Takemura, T.; Baba, H.; Shindo, Y. Excimer Phosphorescence of Naphthalene in Fluid Solution. *Chem. Lett.* **1974**, *3* (9), 1091−1096.

https://doi.org/10.1021/acsaom.2c00106
ACS Appl. Opt. Mater. 2023, 1, 3−9